Supplementary Table 1. Aminoacylation kinetics of *Nm*LeuRS1 for *Nm*tRNA^{Leu}(GAG) and *Nm*tRNA^{Leu}(GAG)-A47cC at 40 ℃[a]

tRNA^{Leu}	K_m (μM)	k_{cat} (s^{-1})	k_{cat}/K_m (mM^{-1} s^{-1})	Activity Ratio
*Nm*tRNA^{Leu}(GAG)	7.73±0.22	(6.40±0.19)×10^{-2}	8.28	1[b]
*Nm*tRNA^{Leu}(GAG)-A47cC	20.2±1.1	(1.24±0.03)×10^{-2}	0.614	0.07

[a] The results are the average of three independent repeats with standard deviations indicated.

[b] The activity of *Nm*LeuRS1 for *Nm*tRNA^{Leu}(GAG) is defined as 1.

A-1

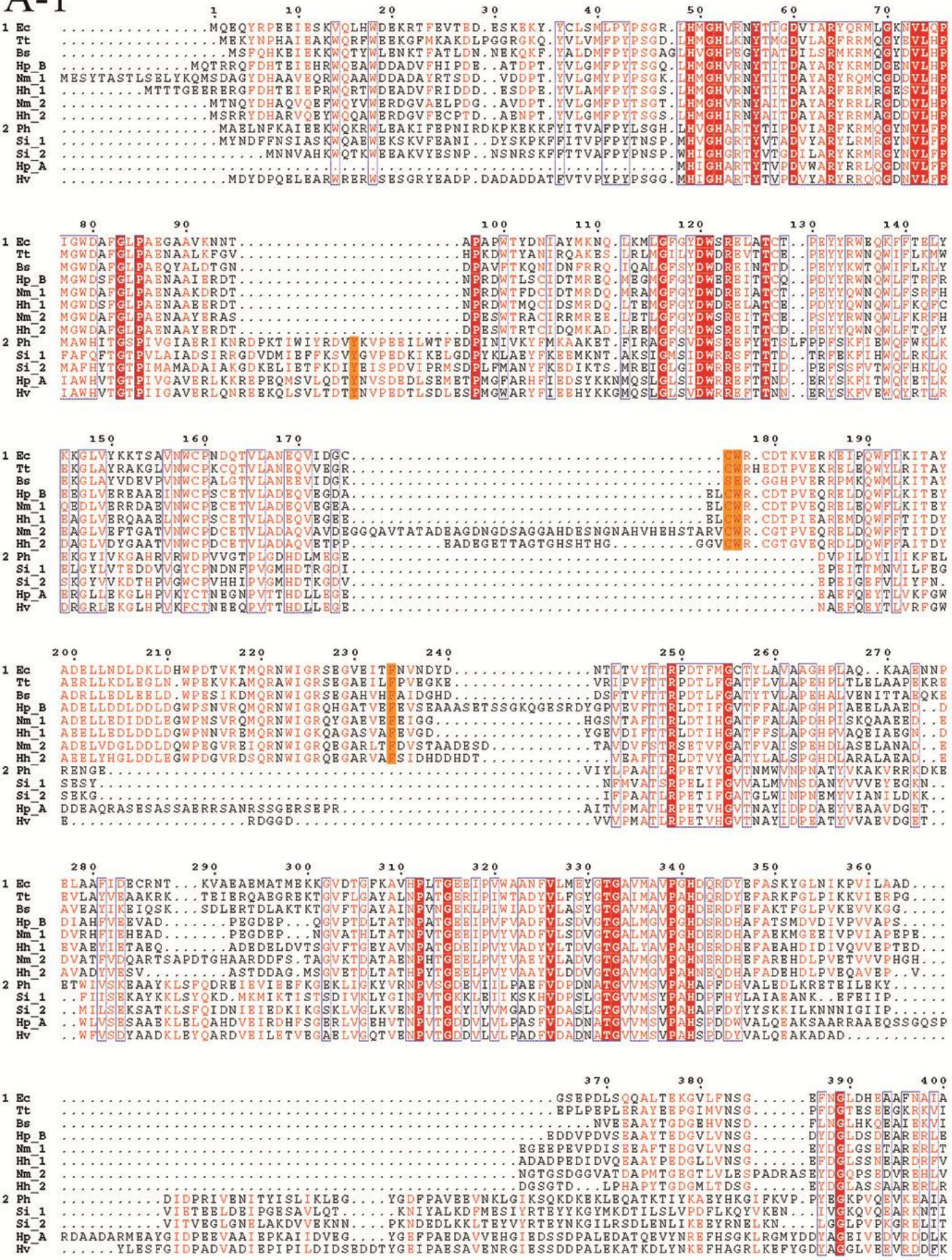

A-2

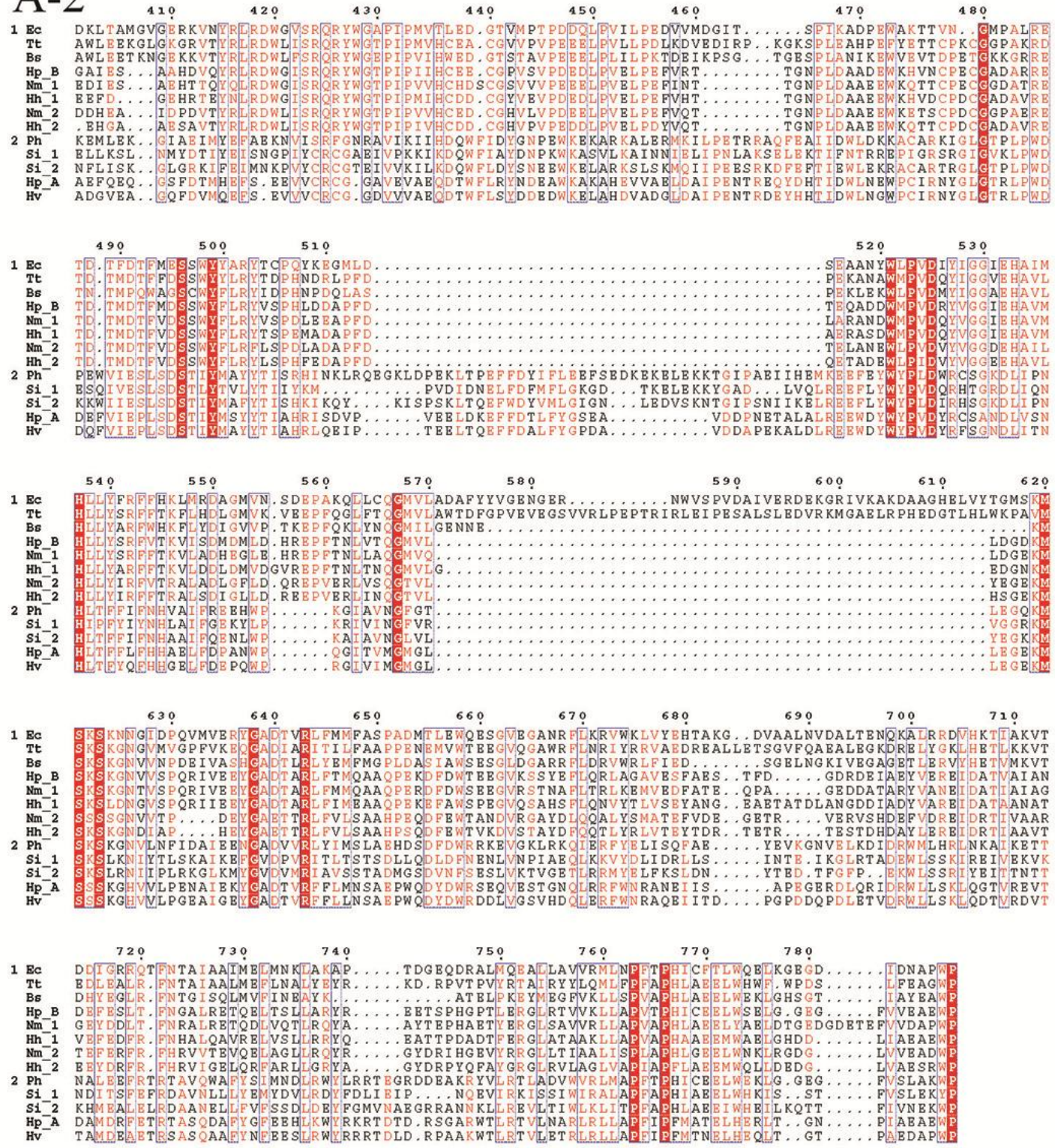

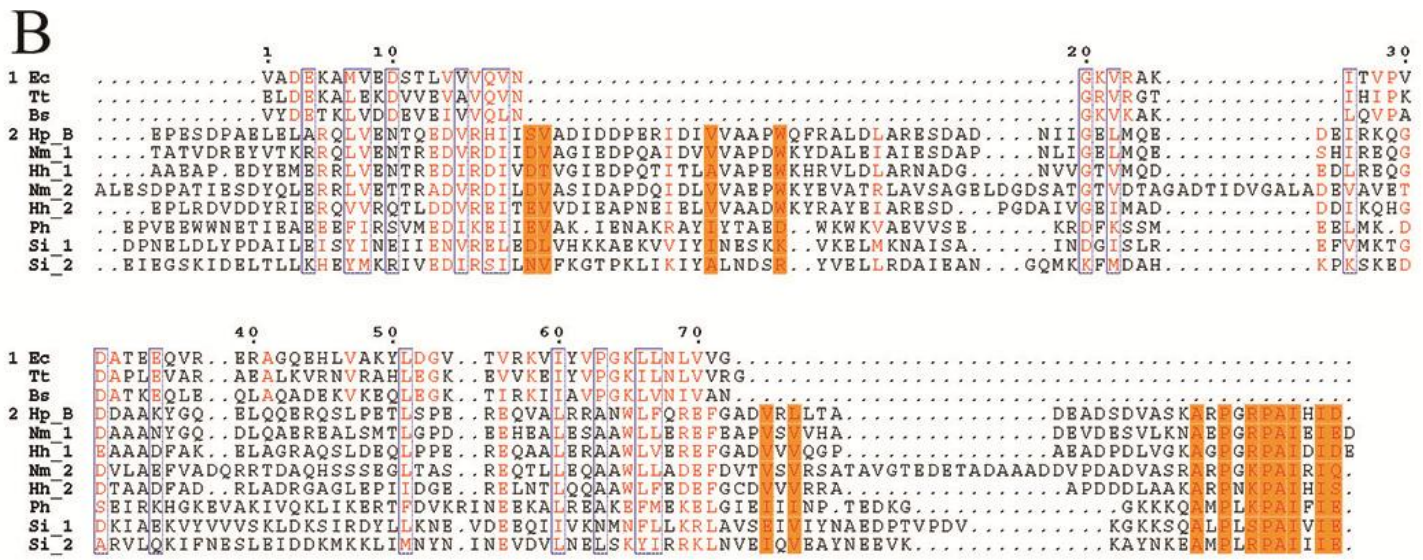

Supplementary Figure 1. Sequence alignment of the N-terminal region (the Rossman fold, CP1, CP2 and α-helix bundle domain) (A) and C-terminal domain (B) of LeuRSs, respectively. Ec, *Escherichia coli*; Tt, *Thermus thermophilus*; Bs, *Bacillus subtilis*; Hp_B & Hp_A, *Haladaptatus paucihalophilus* LeuRS [Bacterial type (accession No. WP_007982262.1) & Archaeal type (accession No. WP_007982263.1)]; Nm_1 & Nm_2, *Natrialba magadii* LeuRS1 & LeuRS2; Hh_1 & Hh_2, *Haloarcula hispanica* LeuRS [LeuRS1 (accession No. YP_004794828.1) & LeuRS2 (accession No. YP_004797622.1)]; Ph, *Pyrococcus horikoshii*; Si_1 & Si_2, *Sulfolobus islandicus* LeuRS [LeuRS1 (accession No. YP_002829648.1) & LeuRS2 (accession No. YP_002829589.1)]; Hv, *Haloferax volcanii*.

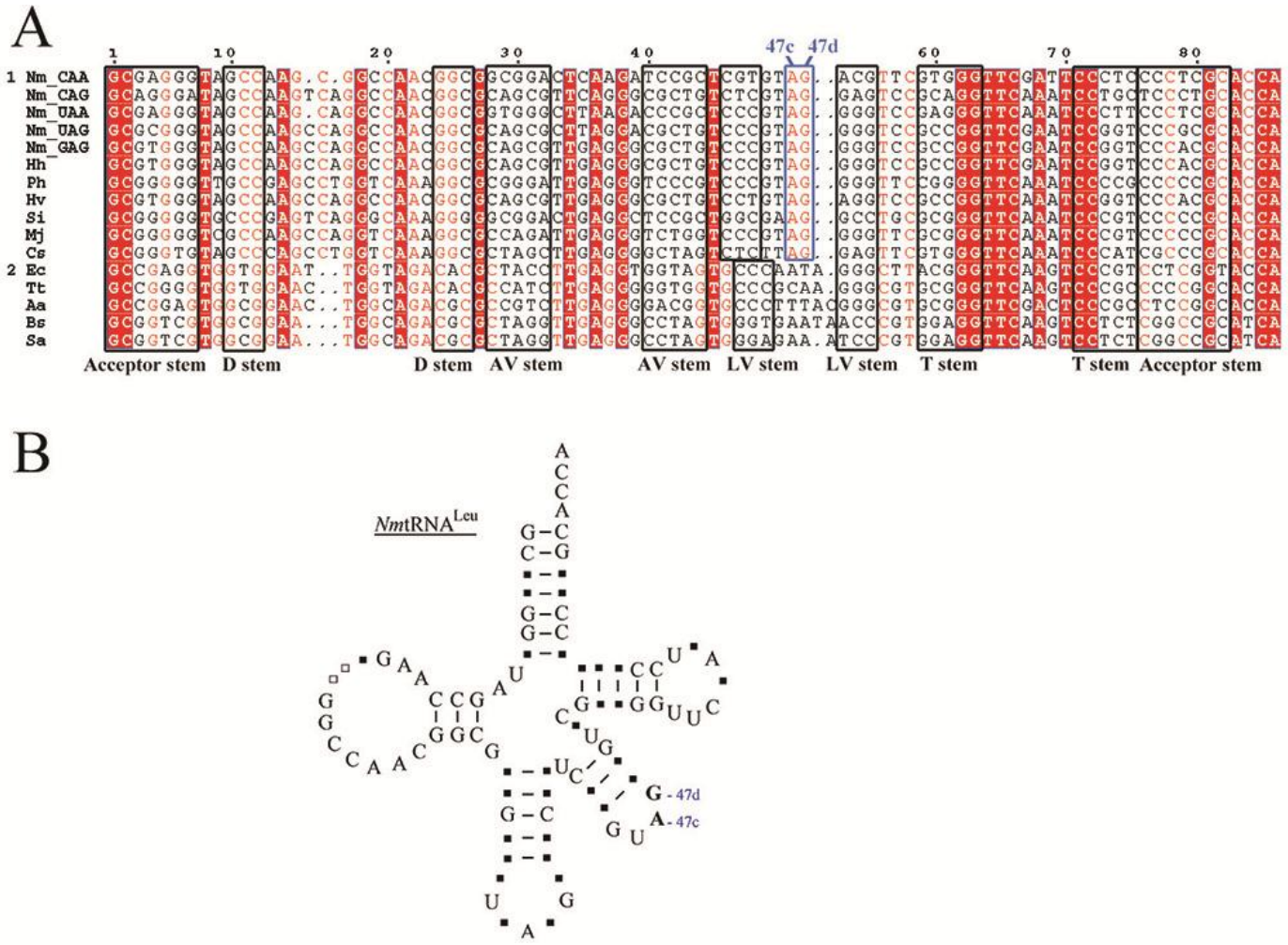

Supplementary Figure 2. *Nm*tRNA^{Leu} are typical archaeal tRNA^{Leu} with conserved A47c and G47d bases. (A) Sequence alignment of all five *Nm*tRNA^{Leu} isoacceptors and tRNA^{Leu}(GAG)s from different species. Nm, *Natrialba magadii*; Hh, *Haloarcula hispanica*; Ph, *Pyrococcus horikoshii*; Hv, *Haloferax volcanii*; Si, *Sulfolobus islandicus*; Mj, *Methanocaldococcus jannaschii*; Cs, *Cenarchaeum symbiosum*; Ec, *Escherichia coli*; Tt, *Thermus thermophilus*; Aa, *Aquifex aeolicus*; Bs, *Bacillus subtilis*; Sa, *Staphylococcus aureus*. Acceptor stem, D stem, AC stem (Anti-codon stem), LV stem (Long variable stem), T stem and the site of 47c, 47d in archaeal tRNA^{Leu} are specified. (B) Cloverleaf structure of *Nm*tRNA^{Leu} with conserved bases specified. The site of A47c and G47d, non-conserved (■) and divergent (□) bases were indicated.

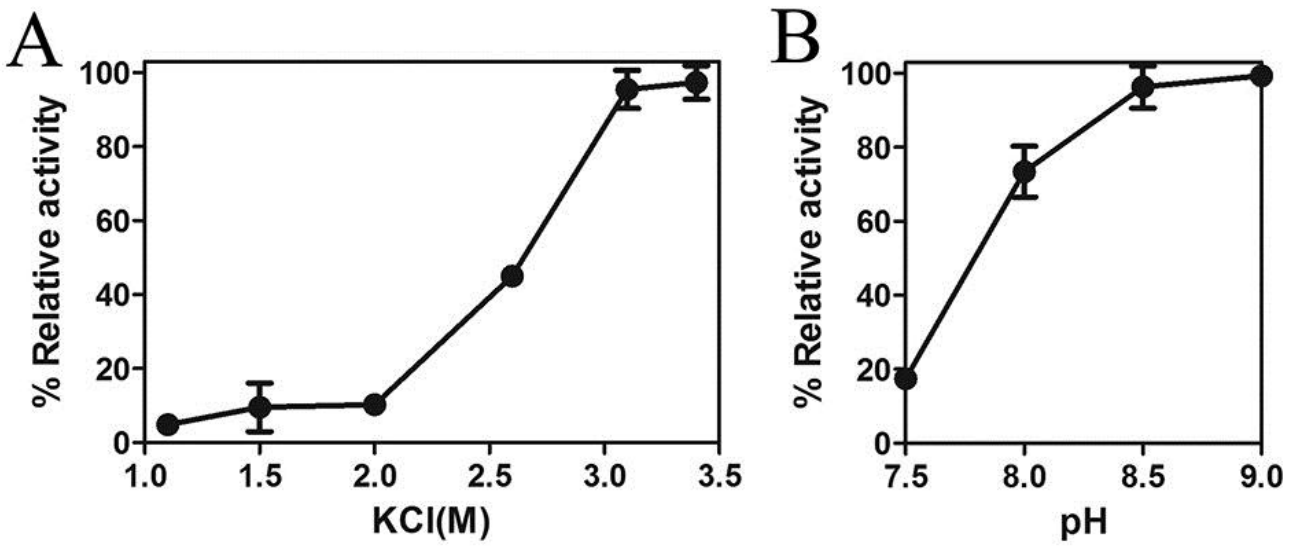

Supplementary Figure 3. Optimization of aminoacylation conditions of *Nm*LeuRS2. (A) Relative aminoacylation activity of *Nm*LeuRS2 under different KCl concentrations (●). The activities of *Nm*LeuRS2 in 3.4 M KCl were defined as 100%; (B) Relative aminoacylation activities of *Nm*LeuRS2 under different pH conditions of Tris-HCl (●). The activity of *Nm*LeuRS2 in Tris-HCl pH9.0 was defined as 100%.

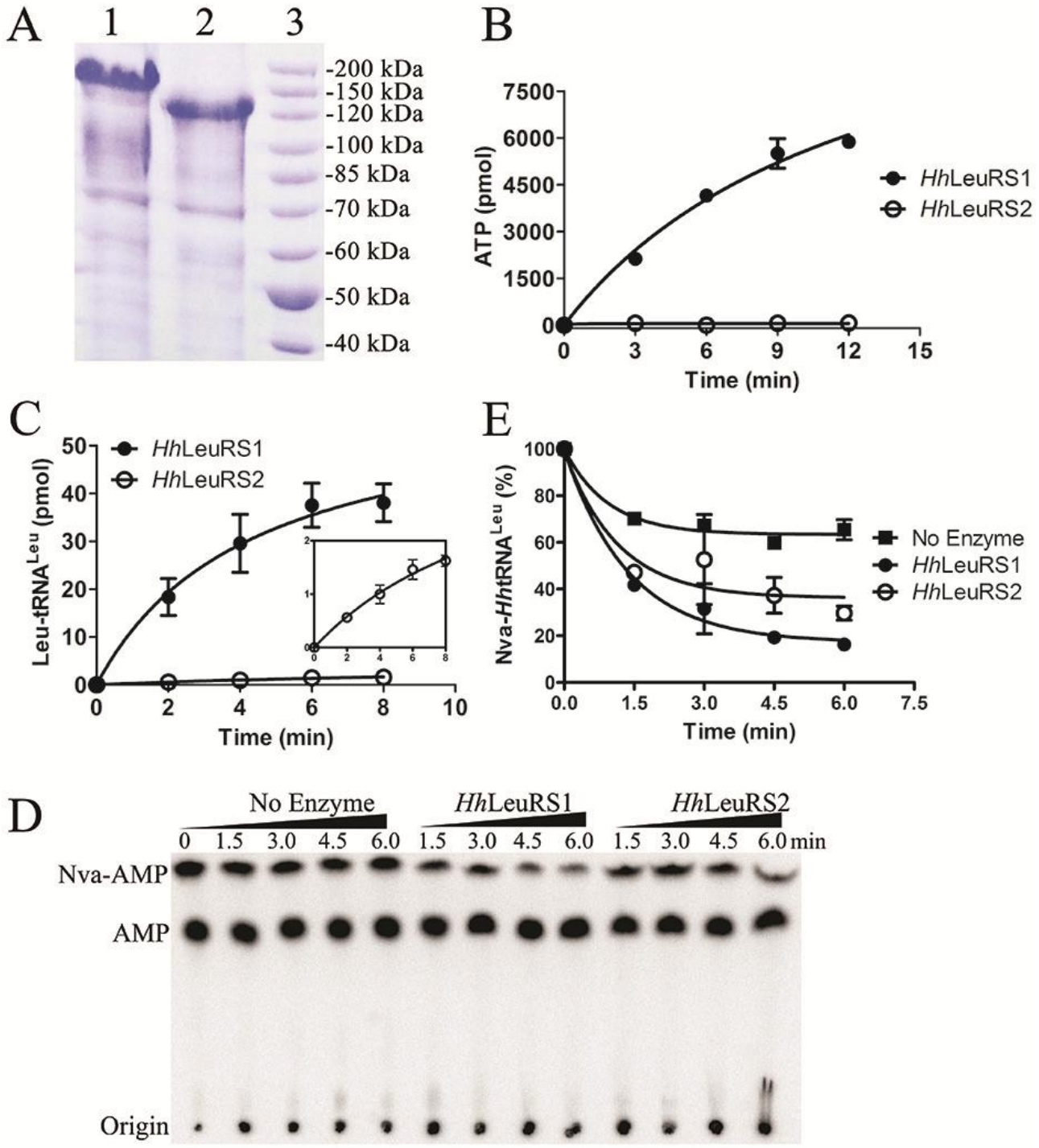

Supplementary Figure 4. *Hh*LeuRS1 showed higher amino acid activation, amino-acylation and post-transfer editing activities than *Hh*LeuRS2. (A) The 10% SDS-PAGE analysis of the purified *Hh*LeuRSs from *E. coli*. Lanes: 1, 2, 3 are *Hh*LeuRS1, *Hh*LeuRS2 and molecular markers (Thermo Scientific, #26614), respectively; (B) The amino acid activation activities of 1 μM *Hh*LeuRS1 (●) and 1 μM HhLeuRS2 (○) for 5mM Leu in pH 8.5, 3.5 M KCl solution; (C) The amino-acylation activities of 400 nM *Hh*LeuRS1 (●) and 400 nM *Hh*LeuRS2 (○) for 4 μM *Hh*tRNA^{Leu}(GAG) in pH 8.5, 3.5 M KCl solution; (D) Representative graph showing the post-transfer editing activity of 500 nM *Hh*LeuRS1 and 500 nM *Hh*LeuRS2 in pH 7.5, 3.5 M KCl solution based on TLC assays; (E) Quantification of the de-acylation activities of *Hh*LeuRS1 (●) and *Hh*LeuRS2 (○) in D.

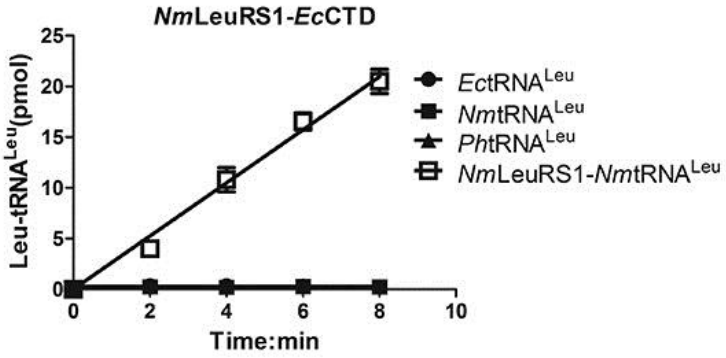

Supplementary Figure 5. The aminoacylation activities of *Nm*LeuRS1-*Ec*CTD for *Nm*tRNA^{Leu} (■), *Ec*tRNA^{Leu} (●) and *Ph*tRNA^{Leu} (▲). The aminoacylation activity of *Nm*LeuRS1 for *Nm*tRNA^{Leu} (□) was used as the positive control.

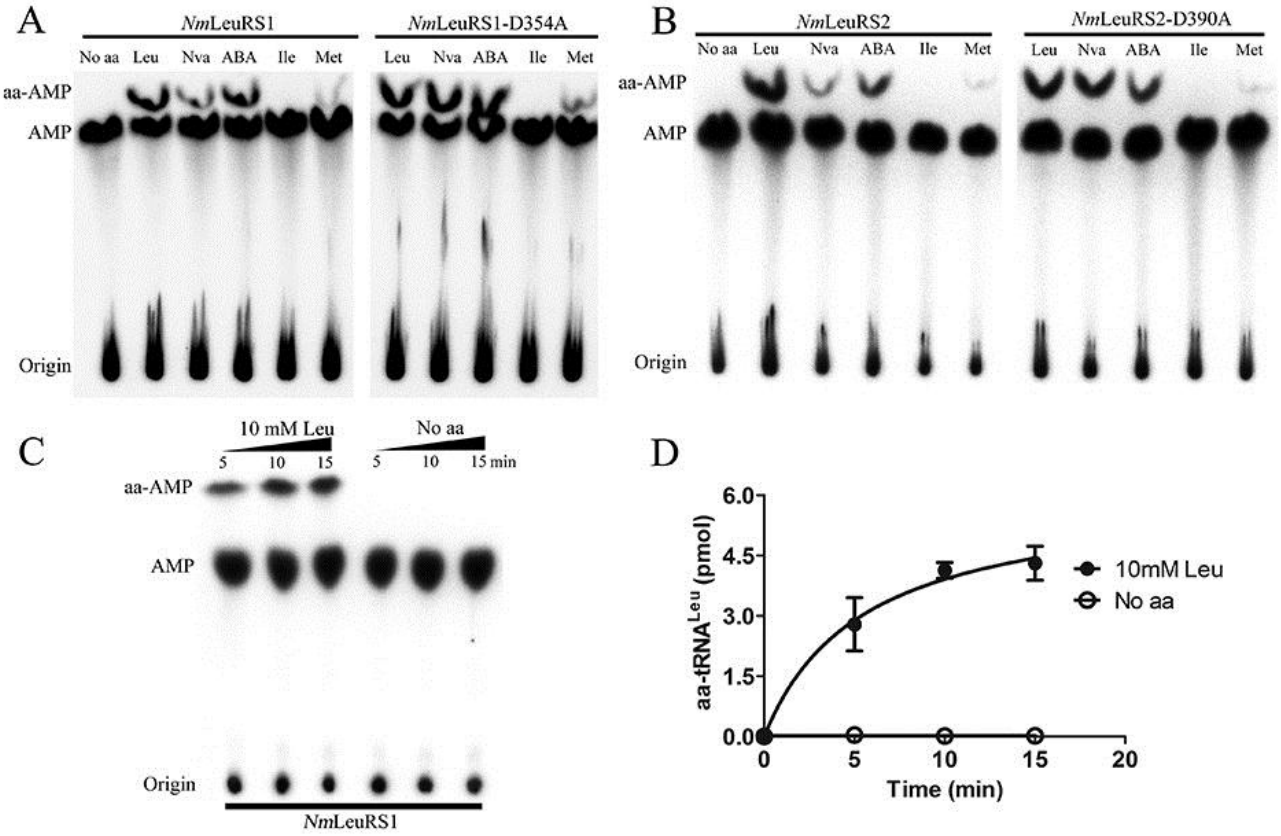

Supplementary Figure 6. The aminoacylation activities of *Nm*LeuRS1 and *Nm*LeuRS1-D354A (A), *Nm*LeuRS2 and *Nm*LeuRS2-D390A (B) for cognate Leu and non-cognate Nva, ABA, Ile and Met based on TLC assays. (C, D) The aminoacylation activities of *Nm*LeuRS1 for Leu and without amino acid (No aa) were used as the positive and negative control, respectively.